Environmental Science and Pollution Research (2021) 28:66340–66354
https://doi.org/10.1007/s11356-021-15274-7

RESEARCH ARTICLE

Textile ageing due to atmospheric gases and particles in indoor cultural heritage

Pauline Uring[1] · Anne Chabas[1] · Stéphane C. Alfaro[1]

Received: 27 January 2021 / Accepted: 29 June 2021 / Published online: 31 July 2021

Abstract

Textile fibre degradation can be due to many factors. The most common cause is light exposure, but upon the lifespan of a textile, many other environmental factors are to be taken into account. This study focuses on the role of atmospheric compounds—both particulate and gaseous species—on natural textiles ageing, more specifically cotton, silk and wool. To achieve this, reference samples of textiles were exposed to contrasted environments (marine, urban and semi-rural museums and historical buildings) for natural ageing. These conditions were also reproduced in an experimental chamber dedicated to the study of the impact of airborne pollutants on heritage materials. Experimental ageing allowed to highlight degradation mechanisms for each fibre: SO_2 and HCOOH cause the cleavage of cotton's glyosidic links and silk's peptide bonds, while NO_2 promotes the oxidation of the fibres. The most harmful pollutant towards cotton is NO_2 since it causes both its oxidation and hydrolysis. The case of wool is more complicated: HCOOH provokes peptide link cleavage (similarly to silk) but this fibre is less sensitive to SO_2 attacks than silk and even seems to be protected against future alterations after having been firstly exposed to this pollutant. In any case, this experimental study evidences that damages caused by gaseous pollutants are fostered by the presence of particles, regardless of the chemical composition of the particle coating.

Keywords Natural fibres · Marine · Terrigenous and anthropogenic particles · Gaseous pollutants · Monuments · Museums · CIME chamber

Introduction

Tapestries, curtains, costumes, hangings, etc. are frequently on display in museums and monuments. These textiles are made mainly from natural fibres, either animal (wool, silk) or vegetal (cotton, flax). Animal fibres are comprised of proteins (keratin in wool, fibroin in silk) while many vegetal fibres are mainly or partly made of cellulose (a polymer repeating cellobiose units). Since these precious artefacts need to be preserved for the longest time and in the best state possible, environmental parameters responsible for their degradation must be closely studied and documented to be able to mitigate their impact.

Light has been the most studied alteration factor for textiles. UV and visible radiations lead to yellowing and bleaching of wool and silk (Ramsay 1970; Launer 1971; Duffield and Lewis 1985; Davidson 1996; Baltova et al. 1998; Koussoulou 1999; Shao et al. 2005; Dyer et al. 2006) as well as embrittlement of the fibres through photooxidation and breakage of disulphide and peptide bonds (Karpowicz 1981; Carr and Lewis 1993; Millington and Church 1997; Tsuge et al. 2000; Kang et al. 2004; Timar-Balazsy and Eastop 2012; Koperska et al. 2015; Kissi et al. 2017). The same radiations are responsible for the yellowing and darkening of cotton (Buschle-Diller and Zeronian 1993; Korenberg 2007) and induce the oxidation of hydroxyl groups oxidation

Highlights The ageing of textiles was studied in French cultural heritage sites with contrasted environments.
Realistic ageing of textiles was reproduced in an experimental chamber.
The SO_2, NO_2 and HCOOH levels in the chamber were derived from the in situ environmental study.
Degradation mechanisms for cotton, silk and wool due to particulate and gaseous species are described.
Low-concentration experiments provide reliable information about ageing of cultural heritage materials.

Responsible Editor: Michel Sablier

✉ Anne Chabas
anne.chabas@lisa.ipsl.fr

[1] Univ Paris Est Creteil and Université de Paris, CNRS, LISA, F-94010 Créteil, France

and glycosidic bonds breakage (Phillips and Arthur 1964; Dupont 1996; Havermans and Dufour 1997; Sistach et al. 1998; Margutti et al. 2008; Credou and Berthelot 2014) of cellulose.

Acids and alkali solutions are also known to lead to fibre degradation. Acidic hydrolysis of cotton is well documented. It is caused by a random chain scission of the polymer (glycosidic bond breakage) and the formation of a carbonyl functional group at the end of the newly formed chain (Whitmore and Bogaard 1994; Zhao et al. 2007; Sun et al. 2007; Timar-Balazsy and Eastop 2012). Cellulose being a semi-crystalline material, degradation first targets amorphous regions but can also affect crystalline regions at further alteration stages (Florian et al. 1991; Koura and Krause 2013). Cotton is more resistant to alkali; such environments lead to the peeling of the cellulose, which is to say the breakage of the last unit of cellobiose. This has a limited impact on the global mechanical resistance of the fibre (Knill and Kennedy 2003; Pavasars et al. 2003). It should be noted that hydrolysis and oxidation of cellulose can happen simultaneously and reinforce each other: oxidation leads to the formation of carboxylic acids that contribute to acidic hydrolysis, and the latter promotes the formation of reducing end groups that foster oxidation (Łojewski et al. 2010). Proteinaceous fibres are also targeted by acids and alkaline solutions. Peptide bonds of silk and wool are hydrolysed by acid attacks that lead to the embrittlement of the fibres; however, disulphide bonds are somewhat resistant to acid hydrolysis (Inglis and Liu 1970; Otterburn 1977; Taddei et al. 2007). Alkaline solutions are less efficient in silk degradation, as only end of chain units are targeted; however, such alteration makes fibres more sensible to future alterations (Shaw 1964; Mellet and Louw 1965). Wool is more easily altered by alkali than silk: disulphide bonds can be broken in such environments, leading to the formation of yellow chromophores and emission of sulphur products (Norton and Nicholls 1967; Brimblecombe et al. 1992; Wojciechowska et al. 1999).

Indoor atmospheric conditions have an impact on textiles that are sensitive to relative humidity (RH) and temperature. As hygroscopic materials, textiles can adsorb water (Fuzek 1985; Bismarck et al. 2002; Hill et al. 2009): the fibres swell and are more plastic (Agarwal et al. 1997; Baley et al. 2005; Iqbal et al. 2012; Timar-Balazsy and Eastop 2012). The weight gain and stretching during water uptake followed by shrinking upon drying causes mechanical stress on the fibres (Lennard and Dulieu-Barton 2014; Bratasz et al. 2015). Temperature rise also increases degradation rates (Michalski 1993; Pawcenis et al. 2016) and high RH boosts the development of microorganisms responsible for multiple damages to textiles (Caneva et al. 1991; Florian 1997; Seves et al. 1998; Szostak-Kotowa 2004; Kavkler et al. 2011).

In indoor polluted atmosphere, gaseous species (carbon dioxide CO_2, nitrogen dioxide NO_2, sulphur dioxide SO_2, acetaldehyde C_2H_4O , formaldehyde CH_2O) can easily be converted into acids (Spicer et al. 1993; Grzywacz 2006; Schieweck and Salthammer 2009; Vichi et al. 2016) and cause fibres hydrolysis (Brysson et al. 1967; Upham and Salvin 1975). However, data on cellulose degradation are available from more studies on papers than on textiles per se: it is known that SO_2 can be adsorbed on cellulosic fibres and acidify them (Hudson and Milner 1961; Edwards et al. 1968; Johansson et al. 2000; Johansson and Lennholm 2000). NO_2 can also acidify cellulose, cause acidic hydrolysis and oxidation as well as discoloration on paper made of cellulose (Miyazaki 1984; Bégin et al. 1999; Menart et al. 2011). As the concentration of volatile organic compounds (VOCs) in the indoor environment can be very high, especially in new buildings (Brown et al. 1994), their impact has also been studied, but again, more on paper than on textiles. VOCs with an acidic or oxidative function can alter cellulose (Strlič et al. 2011). Formic acid (HCOOH) is particularly reactive (Tétreault et al. 2013). Studies on other textiles are scarce; wool and silk can adsorb SO_2 and acidic hydrolysis is possible (Walsh et al. 1977; Kobayashi and Yoshizumi 1994; Timar-Balazsy and Eastop 2012). Moreover, studies targeting specific gaseous pollutants often use high concentration levels of gases to obtain results with a limited exposure time. Such methods have been questioned since the same mechanisms are sometimes not likely to happen at lower concentrations levels, even over longs periods of time (Williams and Grosjean 1992; Adelstein et al. 2003).

Beside gases, particulate matter must also be considered. Aerosols can settle on materials and cause multiple alterations: soiling (Watt and Hamilton 2003; Chabas et al. 2007; Uring et al. 2018), mechanical damage (Tétreault 2003), chemical alterations (Collective 2011; Grau-Bové and Strlič 2013). The specific effect on textiles has yet to be studied; some rare data are available on paper and shows that dust layers contribute to cellulose degradation (Bartl et al. 2016; Grau-Bové et al. 2016) and undergo chemical transformation forming larger efflorescences that penetrate in-between fibres (Uring et al. 2019).

The understanding of textiles' degradation mechanisms in indoor atmosphere remains limited. The role of atmospheric particles in textiles degradation has yet to be defined, as well as the interaction with other environmental parameters like the concentration of gaseous pollutants and microclimatic conditions. This multifactor system must be studied to be able to qualify and quantify the damage induced by such environmental conditions on textiles.

The atmosphere of French museums located in urban, marine and semi-rural areas has been thus characterised. Primary (CO_2, NO_2, HCOOH) and secondary (O_3) pollutants and mixture of halite, mascagnite, soot, clays and calcite particles are characteristic of the studied atmospheres (Uring et al. 2020). This preliminary study allowed to target and set the

parameters of laboratory experiments. These consist of ageing in a lab-made environmental chamber "CIME" injecting both gases and particulate matter in order to reproduce realistic dry atmospheric deposition (Chabas et al. 2015). The aim of this paper is to present the experimental setup combining in situ measurements and laboratory ageing in order to highlight and to monitor, for the first time, the initial step of the evolution of textile fibres exposed to gaseous pollutants alone or in synergy with a mixture of particles.

Materials and methods

Reference materials

Because largely represented in museum and historical monuments, cotton, silk and wool were selected. To guarantee the homogeneity of the sample, colourless, plain-weave and standardised textiles were selected and purchased from EMI-Developpement (Bréviandes, France). The standards were the NF ISO 105-F02 for cotton, the NF ISO 105-F01 for wool and the NF ISO 105-F06 for silk. The surface mass is 115 ± 5 g.m^2, 125 ± 5 g.m^2 and 60 ± 3 g.m^2 respectively. Before use, textiles were thoroughly cut in coupons (6 cm × 6 cm), rinsed with deionized water and dried under laminar air flow.

In situ and laboratory ageing

Textile coupons were displayed in French historical monuments for two years. Three contrasted environments were chosen:

- The Villa Kérylos, located by the Mediterranean Sea (Beaulieu-Sur-Mer),
- The Musée de Cluny, in the urban environment of Paris,
- The Château de Fontainebleau, in a semi-rural environment.

The rooms in Cluny and Fontainebleau have dimmed artificial lighting. At the Villa Kerylos, the rooms are more exposed to natural lighting. The coupons are systematically moved away from the light sources and do not receive direct light radiation.

Half these coupons were withdrawn after six months to be exposed in the CIME chamber whose technical description is presented in (Chabas et al. 2015). The other half of these coupons were left ageing for two years in their respective sites.

Another set of textile coupons were directly exposed inside CIME to be altered following the protocol detailed in Uring et al. 2019. To summarize, atmospheric particles found on site, such as clay, calcite, soot, mascagnite and halite (Uring et al. 2020) were firstly injected in the CIME chamber. Clay and calcite were introduced in the chamber through the SAG410-U dust disperser (Topas-Gmbh). Soot particles were produced by combustion process through a miniCAST 5201A generator (Jing). Mascagnite and halite were generated by atomization of a saline solution using an AGK2000 instrument (Palas).

Textile coupons without particles or with particles (deposited in the CIME chamber or in situ) were then submitted to three distinct gaseous alteration cycles that are detailed in Table 1. No light radiation is applied during the test (darkness).

Environmental conditions were set according to data obtained through the indoor atmosphere study of the Villa Kerylos, the Musée of Cluny and the Château de Fontainebleau (Uring et al. 2020). In this in situ study, temperature, relative humidity, NO_2, O_3, CO_2 and organic solvents (in eq. formaldehyde CH_2O) were measured. For the ageing tests in the CIME chamber, it was decided to inject the acidic form of formaldehyde that is to say formic acid (HCOOH) to accelerate the reactions. Although not detected in today's indoor atmospheres, SO_2 was also chosen to reflect the ancient atmospheres that historic textiles must have experienced. Temperature, relative humidity and CO_2 concentration were maintained constant during the ageing tests.

In concrete terms, SO_2 and NO_2 pollutants were injected directly from pure gas bottles, ozone was produced by a calibration source (2B Technologies Inc.). Gaseous HCOOH obtained by heating the liquid phase was injected thanks to an Adsorbent Tube Injector System (ATIS^{TM}). Dedicated analysers (Envea group) were used to monitor the concentrations of gaseous pollutants in the CIME chamber (AF22M for SO_2, O342M for O_3, AC32M for NO_2, Cairsens for HCOOH, CO12M for CO_2).

Textile coupons analyses

To study the alteration at the molecular levels, all the textiles were analysed with Attenuated Total Reflectance-Fourier Transform Infrared spectroscopy (ATR-FTIR) and Raman spectroscopy.

FTIR analyses were conducted on a Perkin Elmer Frontier equipped with an ATR-diamond/ZnSe crystal accessory; 100 scans were accumulated, with a 4-cm^{-1} resolution over the 4000–550 cm^{-1} range. A constant pressure was applied, ensured by the pressure gauge (maintained at the arbitrary level of 100) during the measurements.

Raman spectra were obtained on a Raman Bruker Senterra with a 785-nm laser, with an Olympus LCPLN50XIR objective and 0.65 for the numerical aperture adapted to IR; the number of accumulations was adapted depending on the studied material, with a 3–5 cm^{-1} resolution. In order to limit florescence phenomena (often less at higher wavelengths for organic compounds), the choice of red laser was preferred.

Table 1 Description of the different artificial ageing experiments in CIME chamber

Gaseous alteration cycle	SO_2+O_3	NO_2+O_3	HCOOH
Temperature	20 °C		
Relative humidity	75 %		
SO_2 level (ppb)	400 injected twice a day	0	
NO_2 level (ppb)	0	Maintained at 1000	0
HCOOH level (ppm)	0		Maintained at 25
O_3 level (ppb)	600 injected twice a day		0
CO_2 level (ppm)	Maintained at 2000		0
Cycle duration	4 weeks	2 weeks	4 weeks

Moreover, before each analysis, the sample was irradiated at the working wavelength for a few seconds (bleaching).

The obtained spectra were then processed with a baseline subtraction on Origin Pro software to improve the spectra reading or to limit the residual fluorescence. In FTIR, the selected anchor points were 1730 and 870 cm^{-1} for silk, 1720 and 895 cm^{-1} for wool. No baseline subtraction was done for cotton. In Raman, the anchor points were 200, 282, 367, 467.5, 600, 800, 1140, 1750, 2250, 2800 and 3140 cm^{-1} for silk, 358, 443, 610, 793, 1143, 1505, 1720 cm^{-1} for wool, 136, 200, 744, 855, 1520, 1750, 2670, 3025 cm^{-1} for cotton.

After baseline removal, a standard normal variate (SNV) pre-processing was applied to the spectra. This reduces the dispersion, particularly within a sample. The spectrum was centred on its mean and normalized by its standard deviation. This explains the sometimes negative values in absorbance scale on the FTIR graphs presented in this paper. These operations were performed on ChemFlow (free online platform).

In some cases, as already evidenced by (Odlyha et al. 2007), the calculation of second derivative spectra (d^2y/dx^2) with Origin Pro made it possible to highlight inflection points and to detect certain spectral bands more easily.

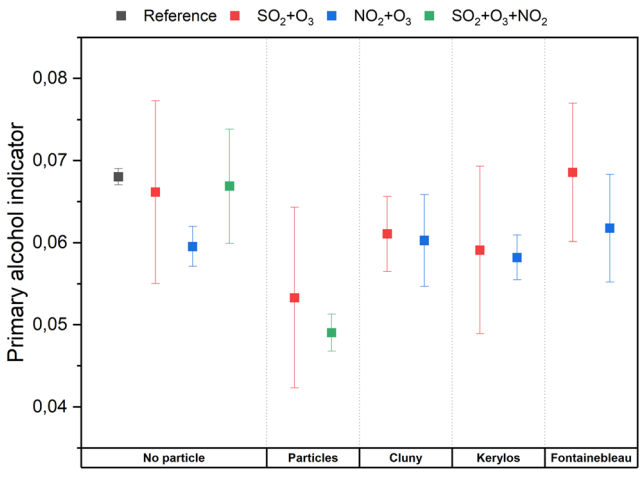

Fig. 1 Primary alcohols indicators on cotton coupons without or with particle coating (deposited in the CIME chamber or in situ during 6 months at Cluny, Kerylos, or Fontainebleau) and then submitted to different gases injected in the CIME chamber

To finish, different indicators were calculated by integrating and measuring the height of the bands of the Raman and FTIR spectra. These operations were performed on Origin Pro. All indicators were calculated for each spectrum and then the values obtained were grouped by sample (spectra acquired at different measurement points) to calculate the mean and standard deviation (indicated by error bars on the graphs). As a reminder, for each sample, 6 Raman spectroscopy and 6 FTIR measurement points were performed.

For cotton, size-exclusion chromatography (SEC) and viscosimetry were also used to have more specific information on the cellulose polymer chain. Following the protocol set up by Dupont 2003, 5 mg cotton samples were dissolved in N,N-dimetyhlacetamide (DMAc) with 8 % lithium chloride. Analyses in SEC-MALS-DRI were conducted as described in Dupont et al. 2018, with a set of three PLgel MiniMIX A columns (20 μm porosity, 250 mm length). Viscosimetry was used to measure the change of intrinsic viscosimetry of cellulose (η). This parameter is linked to the degree of polymerization (DP) of the cellulose chain by the Mark-Howink-Sakurada equation (Evans and Wallis 1987) :

$$DP = (1.1 \cdot \eta)^{\frac{1}{0.85}}$$

Intrinsic viscosimetry was measured following the ISO 5351 protocol. Each sample is represented by a mean indicator (6 measures) and the corresponding standard deviation.

Results and discussion

The spectra obtained in FTIR and Raman all show quite subtle differences between the reference coupons and those altered in situ or in the CIME chamber. Examples are provided as supplementary material for cotton (SM1) and silk (SM2). In order to highlight these fine molecular changes under realistic alteration, the calculations of different indicators have been done for each textile and presented in the following paragraph.

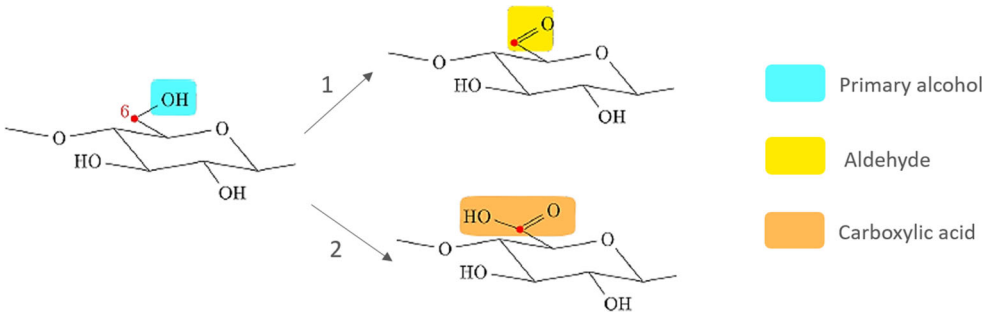

Fig. 2 Two main oxidation reactions of the cellulose without ring opening (adapted from Margutti et al. 2002; Credou and Berthelot 2014)

Cotton damage

Oxidation indicators

Upon cellulose oxidation, carboxyl and carbonyl compounds can form (Łojewska et al. 2005) that are responsible for absorption bands in FTIR at 1730 and 1620 cm^{-1}, respectively (Socrates 2004). The formation of these compounds was difficult to evidence. Firstly, because water bend vibration band overlaps this spectral region and secondly because the 1700–1600 cm^{-1} spectral region is here characterized by a poor S/N ratio that prevents to analyse it with second-derivative spectra.

Thus, oxidation indicators were researched through the presence primary and secondary alcohols. Indeed, cellulose oxidation targets hydroxyl groups and decreases their number. Primary and secondary alcohols can be studied through FTIR and Raman spectroscopy with bands at 1030 and 1055 cm^{-1}, respectively (Castro et al. 2011; Abidi et al. 2014; Hajji et al. 2016). The calculated indicator corresponds to the ratio between the area of the Raman band associated with primary or secondary alcohols and that of the reference at 2900cm^{-1} band.

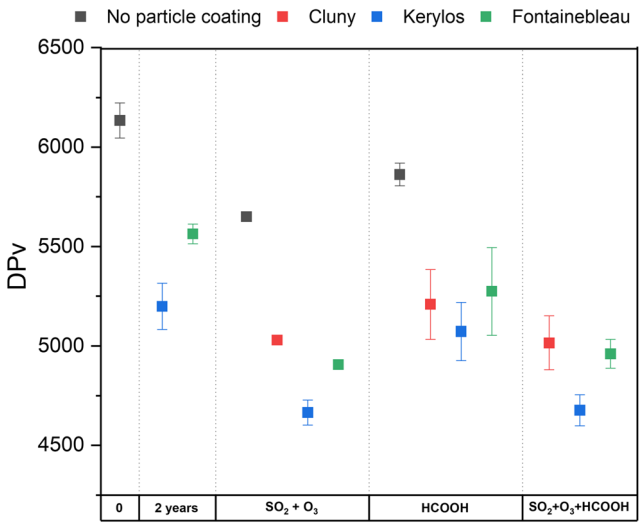

Fig. 3 Degree of polymerisation values (DPv) measured on cotton reference, 2 years in situ exposed coupons and 6 months in situ exposed coupons and then submitted to gaseous pollutants in the CIME chamber

While secondary alcohols show no sign of modification (too important standard deviation), primary alcohol indicators significantly decrease following NO_2 exposure (Fig. 1). This would mean, as suggested in some studies (Sugihara 1953; Camy et al. 2011), that NO_2 attacks selectively the primary alcohol groups through an oxidation of the C6 without pyranose ring opening as illustrated by the following reaction scheme (Fig. 2).

The same indicators show high standard deviations following SO_2 exposure (Fig. 1), making it hard to interpret. However, the most obvious decrease is noted after $SO_2 + O_3$ followed by NO_2 alteration on the coupons covered by particle deposited in the CIME chamber (in green): the particle layer and the gaseous pollutants act as a cocktail effect and foster fibre oxidation.

Hydrolysis indicators

The measurement of the degree of polymerization (DP) was done to highlight cellulose hydrolysis. Because viscosimetry measurements require a large quantity of sample, this technique could only be used on the reference and field samples exposed for 24-month and 6-month and then altered in the CIME chamber (Fig. 3).

For coupons displayed on site for 2 years, a DP loss is already measurable. This DP loss is similar to the DP loss due to aging in the CIME environmental chamber, confirming the realism of the lab-experimentation. Regardless of the gaseous pollutant used for the ageing in the CIME chamber, the decrease of the DP is more pronounced when a coating of particles is present. The Villa Kerylos sample is also the most damaged. The exposition to formic acid of samples previously exposed to SO_2+O_3 does not cause any additional decrease of the DP: multiple alterations do not seem to cause significant hydrolysis.

SEC analyses also allow to retrieve the molar mass distribution of the polymer on reference cotton, without or with particles and exposed to SO_2+O_3 or SO_2+O_3+NO_2 (Fig. 4a). Such analyses allow the calculation of the weight-averaged degree of polymerisation (DP_w). Although the DP_w values are close to those obtained through viscosimetry (and noted

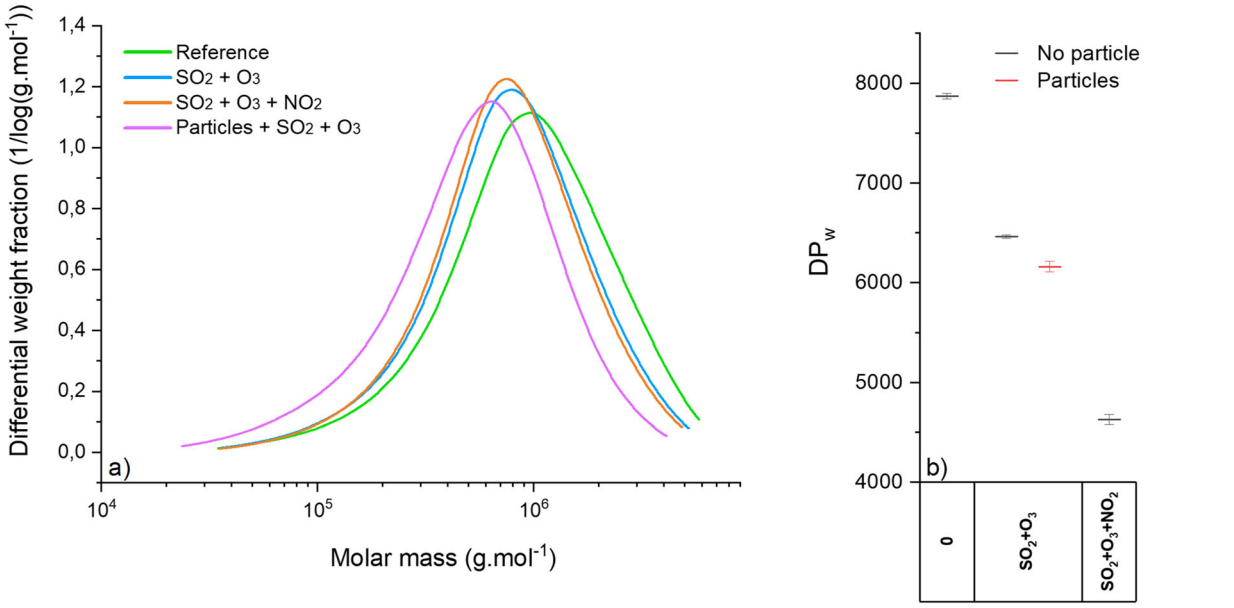

Fig. 4 (a) Examples of weight distribution of polymeric chains of cotton samples without or with particle coating and (b) weight average degree of polymerisation

DP_v to avoid confusion), DP_w and DP_v cannot be compared directly.

Here, the curves show Gaussian shapes whose maximum shifts towards lower molar masses with the simulated alterations. This indicates a DP_w decrease, as confirmed by its calculation (Fig. 4b). The presence of a particle coating leads to a stronger DP_w decrease (about 5 % compared to the sample without particle) upon exposure to SO_2. The attack by NO_2 of the sample without particle already weathered by SO_2 results in a steeper decrease of the DP_w, either due to a higher sensitivity of cotton to this pollutant (Tétreault et al. 2013; Menart et al. 2014) or to a higher speed of degradation considering the pre-altered state of the fibre. All the curves display similar shapes and no secondary peak emerges at lower molar masses.

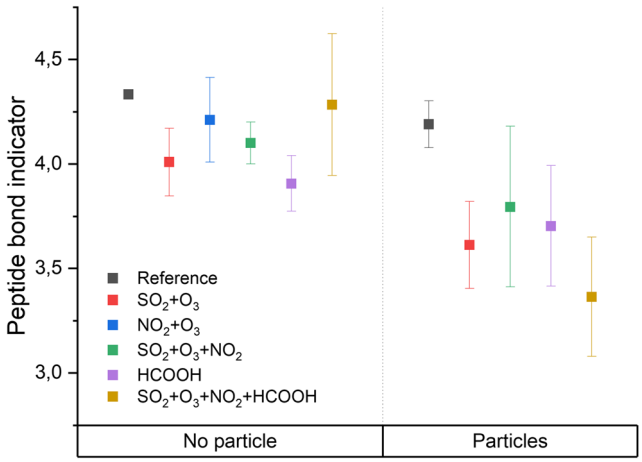

Fig. 5 Peptide bond indicator (FTIR) for silk samples without or with particle coating deposited in the CIME chamber and then submitted to different gaseous pollutants

This can be interpreted by a random attack of the polymer chain (Dupont et al. 2018).

Silk damage

Peptide bond cleavage

Breakage of peptide bonds in silk leads to the embrittlement of the textile (Vilaplana et al. 2015): this phenomenon can happen through hydrolysis or following oxidation. To quantify the eventual breakage of these bonds, the indicator $I_{pep_{silk}} = \frac{P_{AmideIII}}{P_{1442}}$ (area ratio) (Shao et al. 2005) was calculated on the FTIR spectra of the samples. The results (Fig. 5) show that:

- Silk coupons with particle coating show stronger decrease than without,
- $NO_2 + O_3$ only has a limited effect on peptide bonds breakage,
- $SO_2 + O_3$ and HCOOH have similar effects.
- The cumulative effect of $SO_2 + O_3 + NO_2$ + HCOOH + particles is the most effective in breaking peptide bonds.

If carboxyl groups were formed by hydrolysis, a characteristic absorption band would be expected at 1318 cm^{-1} (Koperska et al. 2014); however, no modification is observed in this region of the spectra. This suggests that the hydrolysis is still at a very early stage and that not enough absorbing species have been produced to be measurable by FTIR.

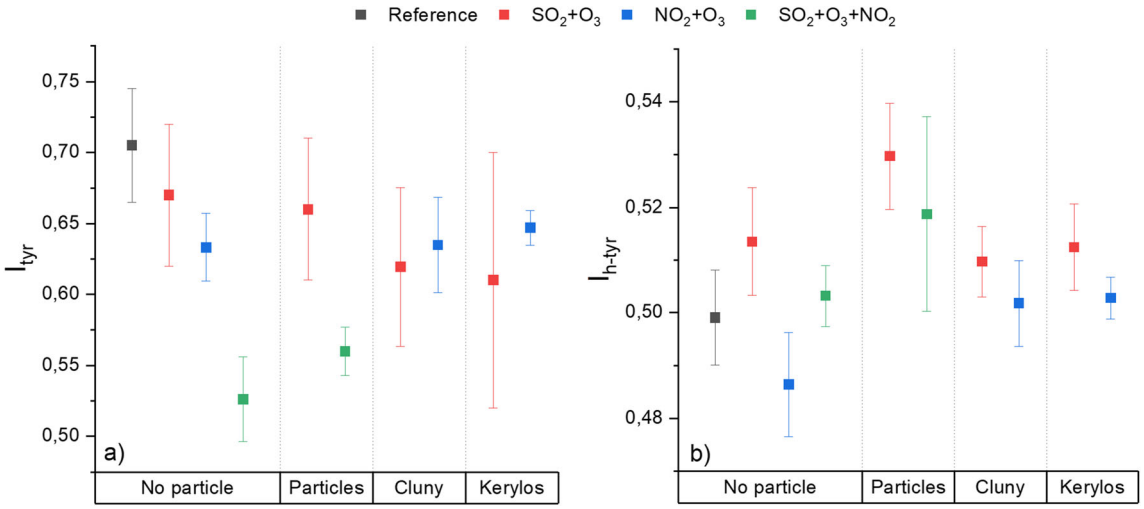

Fig. 6 Tyrosine indicators: (a) tyrosine content and (b) tyrosine exposure for silk samples without or with particle layer deposited in the CIME chamber or in the field (6-month Cluny or Kerylos) and then submitted to gaseous pollutants

Oxidation indicators

Oxidation of the fibres can also occur during their degradation, forming carboxyl or carbonyl groups. Unfortunately, the region around 1735 cm^{-1} on FTIR spectra (carbonyl absorption zone) does not show any absorption band. However, other spectral regions can be affected by the oxidation : the indicator $I_{ox} = \frac{A_{1620}}{} A_{1514}$ (intensity ratio) has already been used to spot oxidation processes (Koperska et al. 2014). In our study, this has not been conclusive: if an oxidation occurred, it must have been light enough to have only little effects on the infrared spectra.

Instead of trying to spot a global oxidation reaction, bands related to specific amino acids found in the protein were studied: in particular, tyrosine showed some evolution. This amino acid is prone to oxidation and photo-oxidation of tyrosine has been widely described (Shao et al. 2005; Timar-Balazsy and Eastop 2012).

This amino acid has a few FTIR (1104, 1165 cm^{-1} (Koperska et al. 2014; Boulet-Audet et al. 2015)) and Raman bands (645, 830, 855, 1165 cm^{-1} (Rousseau et al. 2004; Shao et al. 2005; Koperska et al. 2014)). Two indicators were calculated:

- $I_{tyr} = \frac{P_{850}}{} P_{1450}$ (area ratio of Raman bands), showing the tyrosine content of the fibre (Shao et al. 2005);
- $I_{h-tyr} = \frac{P_{850}}{} P_{830}$ (area ratio of Raman bands), linked to the exposed state of tyrosine residues. This ratio is linked to the hydrogen bonds of the phenoxyl group of tyrosine: a low $I_{h\text{-}tyr}$ means strong hydrogen-bonding, when a higher indicator stands for a more exposed state of the tyrosine (Taddei et al. 2007).

The results are presented in Fig. 6 on in situ (Cluny and Kerylos) or lab-silk coupons without and with particles and then submitted to SO_2, O_3 and NO_2. After being exposed to NO_2+O_3, the tyrosine content decreases; the indicator drops even more when the textile was previously damaged with SO_2+O_3. Indeed, $I_{h\text{-}tyr}$ increases following SO_2 + O_3 exposure, showing that this pollutant makes tyrosine more accessible to further degradation agents. After being exposed to NO_2+O_3, the indicator decreases again, suggesting that surface tyrosine residues were attacked.

Due to the large standard deviations, it is difficult to demonstrate a clear impact of the particles in the reduction of tyrosine content. Nevertheless, tyrosine seems to become more accessible when silk coupons are covered with particles deposited in the CIME chamber.

Wool damage

Disulphide bonds cleavage

Disulphide bonds give mechanical resistance to the wool fibre: their breakage leads to a loss of tensile strength. The S-S bond can be studied through Raman spectroscopy, since it is responsible for bands in the 500–550 cm^{-1} spectral region with intensities and position depending on the conformation of the protein (Wojciechowska et al. 2000; Paquin and Colomban 2007; Barani and Haji 2015). The area of the S-S bond Raman band (500–550 cm^{-1}) was thus calculated and normalized at the 1448 cm^{-1} band (Fig. 7a). Under different gaseous exposures, the intensity of the disulphide vibration band decreases slightly and specially with SO_2. This can be interpreted by a reduction of a small amount of disulphide bonds forming thiol groups by SO_2 as described by Timar-Balazsy and Eastop 2012.

To further understand the impact of SO_2 on the fibres, a closer analysis of the FTIR spectra was conducted between

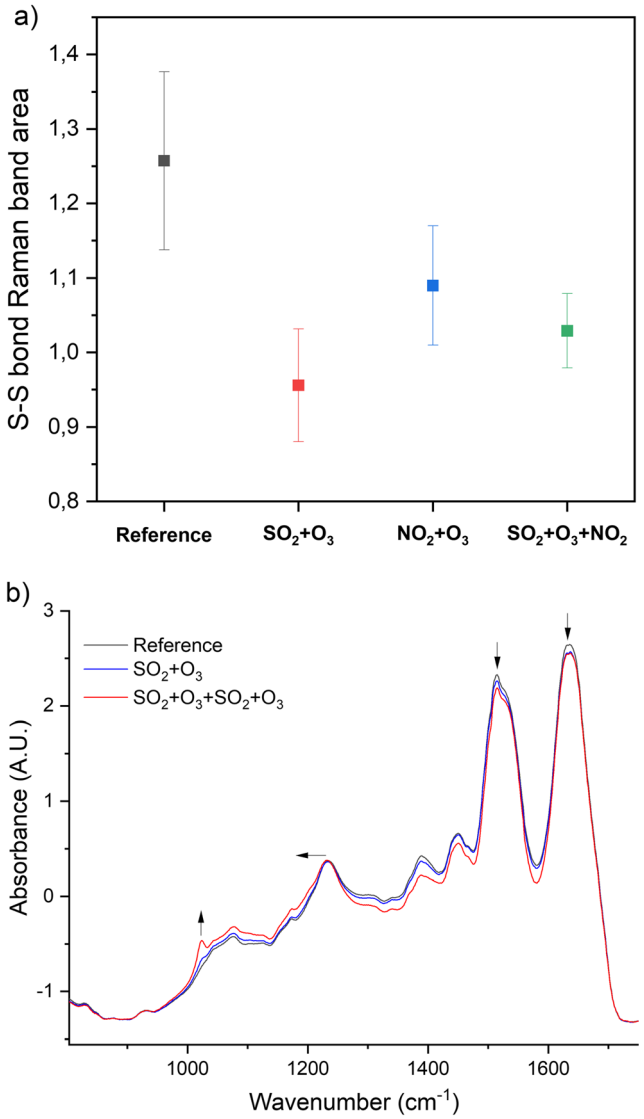

Fig. 7 a Normalized S-S vibration Raman band area (500–550 cm^{-1}) after different gaseous alterations in the CIME chamber. b FTIR spectra of wool exposed to successive SO_2 + O_3 alterations. b. FTIR spectra of wool exposed to successive SO_2 + O_3 alterations

800 and 1700 cm^{-1} (Fig. 7b). Upon SO_2 + O_3 exposure, the amide III band (1230 cm^{-1}) is distorted and widens towards lower wavenumbers, probably due to modifications of hydrogen bonds in the keratin (Odlyha et al. 2007).

A new absorption band also appears at 1023 cm^{-1}. This band is associated to the Bunte salt (S-sulphonate) whose formation is well documented upon wool oxidation (Carr and Lewis 1993; Douthwaite et al. 1993; Millington and Church 1997; Kissi et al. 2017). However, here the formation of this product is specific to the SO_2 exposure; it cannot be caused by the ozone also injected in the chamber since this band does not appear following exposure to the combination of NO_2 and O_3. This suggests another mechanism: cystine sulfitolysis (Gómez et al. 1995; Erra et al. 1997; Posati et al. 2016), which leads to the reversible breakage of disulphide bonds without diminishing the molecular weight of the fibre.

Peptide bonds cleavage

Peptide bonds form the backbone of the protein structure: their breakage would lead to a decrease in the amide bands of the FTIR spectra. The area of the amide I band was calculated and normalized at the 1442 cm^{-1} band following the procedure described by (Odlyha et al. 2007).

The results are presented in Fig. 8 for wool coupons without or with particle layers deposited in the CIME chamber or after 6 months in Cluny, Kerylos and Fontainebleau and then exposed to different run of gaseous pollutants. All pollutants lead to a decrease in absorbance from the amide I band and in particular:

- NO_2 + O_3 has little effect, except for the textile exposed at Kerylos;
- Formic acid seems to be the most aggressive pollutant, notably when combined with particle deposited in the CIME chamber;
- Consecutive alterations on the same textile seem to have less impact than on new textiles: in particular, textiles exposed to formic acid undergo a strong peptide bonds breakage (shown by the decrease of the indicator), whereas the same alteration of textiles previously exposed to SO_2 + O_3 show little modifications.

This might be due to some modifications of the wool fibre provoked by these pollutants; since the textiles exposed to SO_2+ O_3 are supplemented in Bunte salts and thiolates, formic acid could protonate these functional groups rather than attacking peptide bonds.

Neoformed phases

Neoformed phases have been detected on wool coupons exposed in the CIME chamber under formic acid flow. Two bands are notably modified on the FTIR spectra (Fig. 9): at 1343 cm^{-1}, a band appears and at 1386 cm^{-1}, a decreasing of the intensity of the band is noticed.

Formic acid absorbs at 1333 cm^{-1} and formates absorb around 1340 cm^{-1} (Al-Hosney et al. 2005): the 1343 cm^{-1} band could thus be assigned to the formation of formate salts on the wool. Because this band is also present on reference samples, it can be due to reaction of formic acid with impurities. Indeed, the presence of sodium for example is likely due to past wool treatment.

The 1386 cm^{-1} band is assigned to the serine OH bending vibration. It is known that formic acid can react with hydroxyl groups of amino acids to form esters (Hietala et al. 2016);

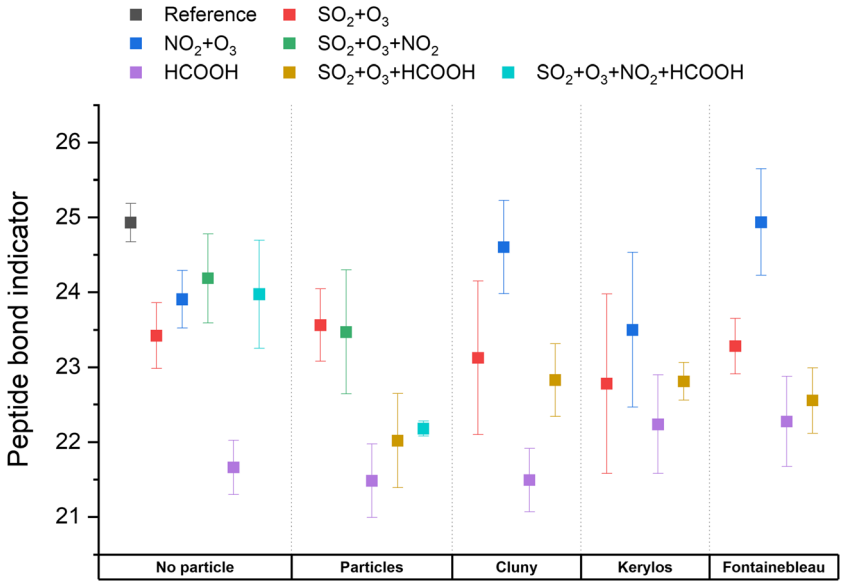

Fig. 8 Peptide bond indicator for wool coupons without or with particle coating deposited in the CIME chamber or in the field at Cluny, Kerylos, or Fontainebleau and then exposed to different gaseous pollutants

however, this hypothesis seems unlikely since the characteristic bands of esters are not present on the spectra (around 1200 cm^{-1} in particular) (Socrates 2004). The serine decrease could also be due to the ability of formic acid to penetrate the fibre's structure and dissolve the amines (Barone and Schmidt 2006): this hypothesis is backed by the peptide bonds breakage induced by formic acid (cf. Peptide bonds cleavage section).

Wool yellowing

Wool yellowing can happen through degradation, by the formation of chromophore species like deshydroalanine following the acid hydrolysis of amine groups of asparagine and glutamic acid. This component absorbs in the infrared region at 876 cm^{-1} (Carr and Lewis 1993; Gómez et al. 1995). It is thus possible to monitor the formation of deshydroalanine through the indicator $I_{yellowing} = \frac{P_{876}}{P_{1442}}$ (band area ratio) as it is presented in Fig. 10.

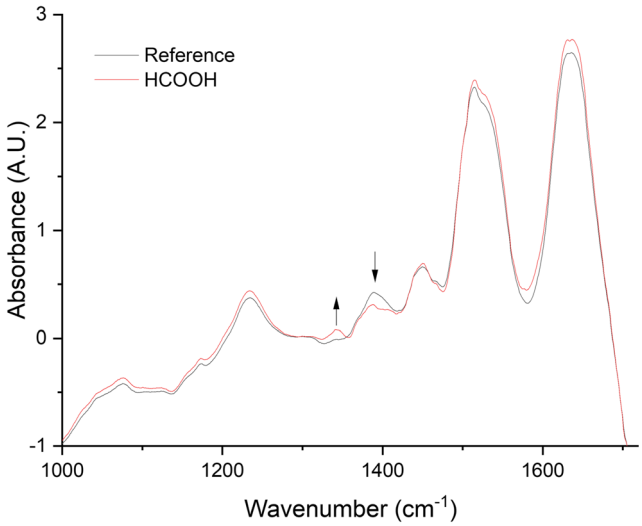

Fig. 9 Example of wool FTIR spectra before and after formic acid exposure in the CIME chamber

On wool coupons without particle coating, only a slight rise is noticeable after the gaseous alterations. Coupons wit particle coating show a higher rise following formic acid exposition. Yellowing of the wool is so only at its origination and not yet perceivable at a macroscopic scale, but it is boosted by the presence of a layer of particles, be it deposited in the CIME chamber or in situ in the field (Cluny, Kerylos or Fontainebleau).

Oxidation indicators

Lipids on the surface of wool can be oxidized to fatty acids, forming carbonyl compounds absorbing in the 1715–1725 cm^{-1} region (Odlyha et al. 2007); however, no band appears around these wavenumbers after the different alterations, so no sign of lipids oxidation can be detected at this stage.

Tyrosine and tryptophan can form yellow chromophores upon oxidation (band at 1161 cm^{-1} in FTIR (Carr and Lewis 1993)) but again, no band is formed in this spectral region following ageing. Raman spectroscopy also allows to study the tyrosine content (830 and 850 cm^{-1}), in a similar manner to silk. However, the ratio $I_{h-tyr} = \frac{P_{850}}{P_{830}}$ is equal to 1.5 and constant: tyrosine is accessible but not modified through the alterations.

Cystine is susceptible to be oxidized. Its photooxidation pathway is well documented and can be studied thanks to the S-O vibration region on FTIR spectra (Carr and Lewis 1993):

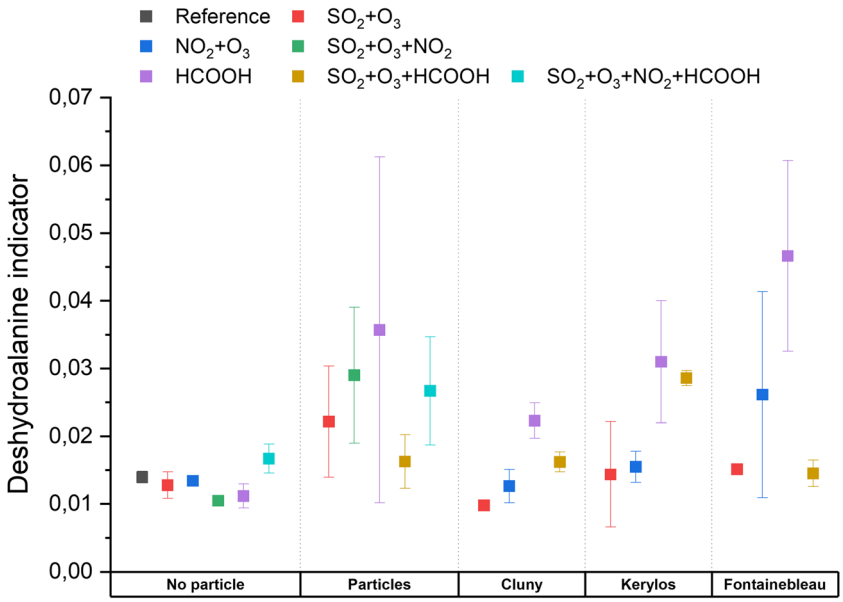

Fig. 10 Deshydroalanine indicator on wool samples without or with particles deposited in the CIME chamber or after 6-month exposure at Cluny, Kerylos and Fontainebleau and then submitted to different gaseous pollutants

– Cystine monoxide (1071 cm^{-1}),
– Cystine dioxide (1121 cm^{-1}),
– Cysteic acid (1040 cm^{-1}) and Bunte salt (1022 cm^{-1}).

From FTIR spectra (Fig. 11a), second-derivative spectra (Fig. 11b) are calculated in order to separate the different bands and identify their formation easily. Following NO_2 + O_3 exposure, a slight increase of the intensity of the 1040 cm^{-1} band (see the pink zone in Fig. 11) is noticeable, denoting the formation of cysteic acid. However, no other intermediate oxidation product is found. The second-derivative spectra confirm the increase and show that more cysteic acid is formed on samples with a layer of particles.

To determine whether these differences are significant, the intensity of the second-derivative is used to take into account only the contribution of the band A indicated in Fig. 11b. The results are presented in Fig. 12. The second-derivative analysis shows most significantly an increase in the cysteic acid band. This increase is favoured on textiles exposed at each site.

The presence of cysteic acid implies the breaking of disulphide bridges: this had been demonstrated in very low proportions (§ 3.3.1). Indeed, the increase in the cysteic acid band is very limited: the oxidation induced by NO_2 is progressive and leads to few cystine breaks.

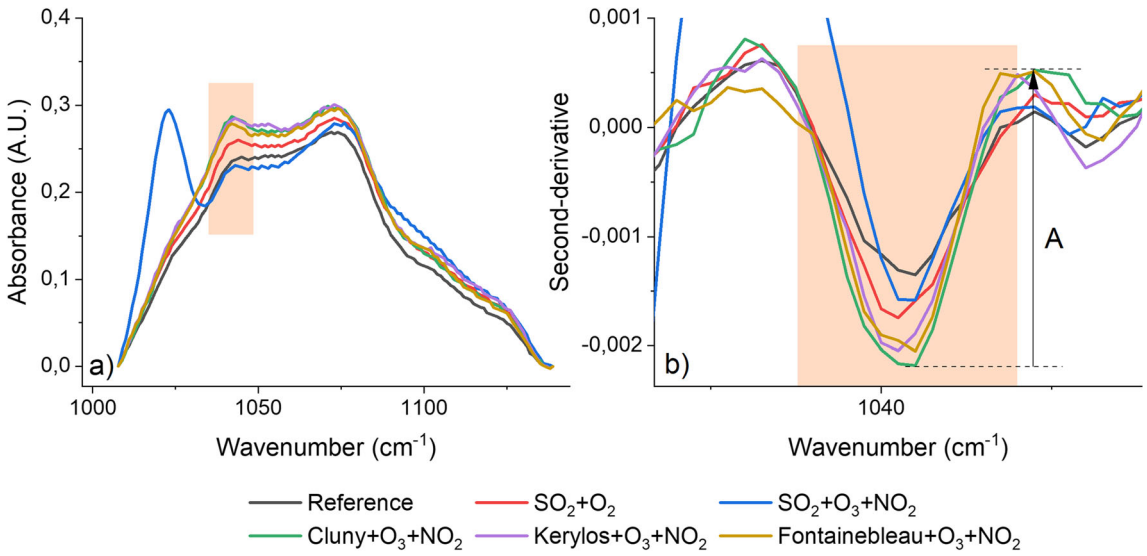

Fig. 11 (a) S-O FTIR band and (b) associated second-derivative spectra of wool coupons without or with particles deposited in the field and then exposed to gaseous pollutants in the CIME chamber

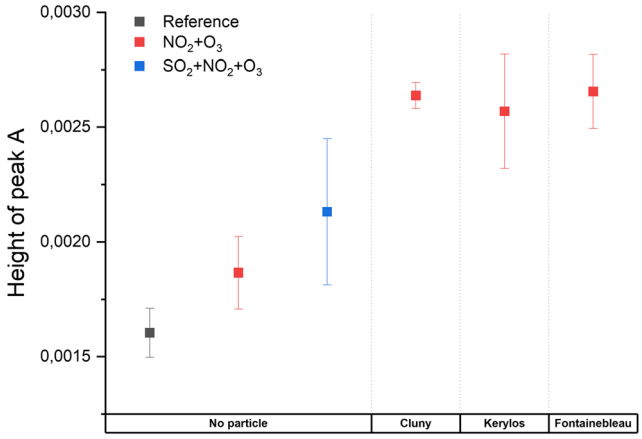

Fig. 12 Comparison of the peak height "A" at 1040 cm^{-1} of wool coupons without or with particles deposited in the field and then exposed to gaseous pollutants in the CIME chamber

Thus, the presence of a deposit of particles, whose chemical composition seems to have little influence, favours the oxidation of wool by NO_2.

Conclusion

Textiles are widely exhibited in museums and monuments where the indoor atmosphere, which is difficult to control, contains potential agents of aggression. However, the role of these atmospheric compounds—both gaseous and particulate—in the ageing of textiles is not well known. In order to document this aspect, an original research combining on-site exposure and ageing in environmental chamber has been carried out on cotton, silk and wool coupons. Three French sites with contrasted atmospheres were chosen: the Cluny Museum in Paris (urban), the Château de Fontainebleau (semi-rural) and the Villa Kerylos (marine). The environmental data measured from these sites helped to parameterise the experiments in the CIME simulation chamber. By combining both particle and gas deposition, these experiments were able to reproduce a very realistic ageing process.

The major results show that each textile has a specific degradation path that depends on the pollutant studied. The presence of a particle deposit eases the alteration of textiles.

In particular, cellulose hydrolysis (regardless of the pollutant used – SO_2+O_3, NO_2+O_3, HCOOH) is stronger in the presence of a particle layer. NO_2 +O_3 selectively oxidises cotton and causes a hydrolysis stronger than SO_2 +O_3; the combination of these two degradation mechanisms makes NO_2 the most aggressive pollutant towards cotton.

Silk on the other hand is the most vulnerable to SO_2 +O_3 and HCOOH that attack its peptide bonds with a higher rate in the presence of a particle coating.

Finally, wool showed many degradation paths. SO_2 +O_3 has a limited impact on the peptide bonds breakage but provokes sulfitolysis. Also, wool seems to be passivated following the exposure to this pollutant, making further degradations less impactful. NO_2 +O_3 oxidises the fibres, leading to disulphide bonds breakage. Formic acid has the highest impact on peptide bonds breakage since it reacts with amino acids and potentially forms formates. The presence of a particle coating fosters oxidation by NO_2 +O_3 and peptide bonds breakage.

The majority of degradation mechanisms are boosted when the textile presents a particle coating, regardless of its chemical composition (urban, rural, marine) at this alteration stage. A slight preferred degradation of the Kerylos sample (marine aerosols) could be explained by the stronger presence of deliquescent salts (especially halite) in this type of particles, more likely to form local liquid phases into which pollutants could dissolve and react more easily with the underlying fibres.

This study has also shown that fibres with particle layers undergo irreversible alterations in short amount of time: after only two years, cotton shows a loss in DP. Two years is very short in the lifespan of a textile exposed indoor in museum and monuments, and is also smaller than the usual cleaning frequency performed in cultural heritage where fragile textiles are cleaned every 5 or 10 years. It is therefore necessary to limit the deposition of particles by acting on their emission source and by removing regularly the particle layers to avoid the formation of particulate mixtures that are reactive to gaseous pollutants, air humidity and ultimately harmful to textiles.

Supplementary Information The online version contains supplementary material available at https://doi.org/10.1007/s11356-021-15274-7.

Acknowledgements The authors are particularly grateful to Béatrice de Chancel-Bardelot (Cluny Museum), Vincent Cochet (Château de Fontainebleau), Christophe Niedziocha and Caroline Bahuau (Centre des Monuments Nationaux / Villa Kérylos). By opening the doors of their monuments and allowing the authors to set monitoring devices and collect samples, they made this study possible.

The authors want to thank Dr. Anne-Laurence Dupont (CRCC, CNRS, MNHN), Pr. Ludovic Bellot-Gurlet (Monaris, Sorbonne University), Dr. Mohamed Dallel (LRMH) and Pr. Laurent Ibos (CERTES, University Paris Est of Creteil) for the accesses to analytical techniques (SEC, Raman and FTIR spectroscopy) and helpful discussions.

The «Direction Régionale des Affaires Culturelles Provence-Alpes Côte d'Azur » (DRAC PACA), the « Etablissement Public château de Fontainebleau » and the « Direction Générale des Patrimoines (DGP) - Ministère de la Culture » which have supported this research are also acknowledged.

Author contribution AC and SA supervised the study. AC and PU performed sampling, on-site manipulation and lab-experiment. AC and PU wrote the manuscript. SA revised the manuscript. All authors read and approved the final manuscript.

Data availability Data and materials can be available on request from the authors.

Declarations

Ethics approval The authors followed the rules of good scientific practice.

Consent to participate Not applicable

Consent for publication Not applicable

Competing interests The authors declare no competing interests.

References

Abidi N, Cabrales L, Haigler CH (2014) Changes in the cell wall and cellulose content of developing cotton fibers investigated by FTIR spectroscopy. Carbohydr Polym 100:9–16. https://doi.org/10.1016/j.carbpol.2013.01.074

Adelstein P, Zinn E, Reilly J (2003) Effect of atmospheric pollution on paper stability. J Pulp Pap Sci 29:21–28

Agarwal N, Hoagland DA, Farris RJ (1997) Effect of moisture absorption on the thermal properties of Bombyx mori silk fibroin films. J Appl Polym Sci 63:401–410. https://doi.org/10.1002/(SICI)1097-4628(19970118)63:3<401::AID-APP17>3.0.CO;2-2

Al-Hosney HA, Carlos-Cuellar S, Baltrusaitis J, Grassian VH (2005) Heterogeneous uptake and reactivity of formic acid on calcium carbonate particles: a Knudsen cell reactor, FTIR and SEM study. Phys Chem Chem Phys 7:3587–3595. https://doi.org/10.1039/B510112C

Baley C, Morvan C, Grohens Y (2005) Influence of the Absorbed Water on the Tensile Strength of Flax Fibers. Macromol Symp 222:195–202. https://doi.org/10.1002/masy.200550425

Baltova S, Vassileva V, Valtcheva E (1998) Photochemical behaviour of natural silk—I. Kinetic investigation of photoyellowing. Polym Degrad Stab 60:53–60. https://doi.org/10.1016/S0141-3910(97)00016-5

Barani H, Haji A (2015) Analysis of structural transformation in wool fiber resulting from oxygen plasma treatment using vibrational spectroscopy. J Mol Struct 1079:35–40. https://doi.org/10.1016/j.molstruc.2014.09.041

Barone JR, Schmidt WF (2006) Effect of formic acid exposure on keratin fiber derived from poultry feather biomass. Bioresour Technol 97:233–242. https://doi.org/10.1016/j.biortech.2005.02.039

Bartl B, Maskova L, Paulusova H et al (2016) The effect of dust particles on cellulose degradation. Stud Conserv 61:203–208. https://doi.org/10.1179/2047058414Y.0000000158

Bégin P, Deschâtelets S, Grattan D et al (1999) The Effect of Air Pollutants on Paper Stability. Restaurator 20:1–21. https://doi.org/10.1515/rest.1999.20.1.1

Bismarck A, Aranberri-Askargorta I, Springer J et al (2002) Surface characterization of flax, hemp and cellulose fibers; Surface properties and the water uptake behavior. Polym Compos 23:872–894. https://doi.org/10.1002/pc.10485

Boulet-Audet M, Vollrath F, Holland C (2015) Identification and classification of silks using infrared spectroscopy. J Exp Biol 218:3138–3149. https://doi.org/10.1242/jeb.128306

Bratasz L, Łukomski M, Klisińska-Kopacz A, Zawadzki W, Dzierżęga K, Bartosik M, Sobczyk J, Lennard FJ, Kozłowski R (2015) Risk of climate-induced damage in historic textiles. Strain 51:78–88. https://doi.org/10.1111/str.12122

Brimblecombe P, Shooter D, Kaur A (1992) Wool and reduced sulphur gases in museum air. Stud Conserv 37:53–60. https://doi.org/10.1179/sic.1992.37.1.53

Brown SK, Sim MR, Abramson MJ, Gray CN (1994) Concentrations of volatile organic compounds in indoor air – a review. Indoor Air 4:123–134. https://doi.org/10.1111/j.1600-0668.1994.t01-2-00007.x

Brysson RJ, Trask BJ, Upham JB, Booras SG (1967) The effects of air pollution on exposed cotton fabrics. J Air Pollut Control Assoc 17:294–298. https://doi.org/10.1080/00022470.1967.10468981

Buschle-Diller G, Zeronian SH (1993) Weathering and photodegradation of cellulose. In: ACS Symposium Series, vol 531. Photochemistry of Lignocellulosic Materials, Chapter 14, pp 177–189. https://doi.org/10.1021/bk-1992-0531.ch014

Camy S, Letourneau J-J, Condoret J-S (2011) Experimental study of high pressure phase equilibrium of (CO2+NO2/N2O4) mixtures. J Chem Thermodyn 43:1954–1960. https://doi.org/10.1016/j.jct.2011.07.007

Caneva G, Nugari MP, Salvadori O (1991) Biology in the conservation of works of art. ICCROM, International Centre for the Study of the Preservation and the Restoration of Cultural Property. Available on https://www.iccrom.org/fr/publication/biology-conservation-works-art

Carr CM, Lewis DM (1993) An FTIR spectroscopic study of the photodegradation and thermal degradation of wool. J Soc Dye Colour 109:21–24. https://doi.org/10.1111/j.1478-4408.1993.tb01496.x

Castro K, Princi E, Proietti N, Manso M, Capitani D, Vicini S, Madariaga JM, de Carvalho ML (2011) Assessment of the weathering effects on cellulose based materials through a multianalytical approach. Nucl Inst Methods Phys Res B 269:1401–1410. https://doi.org/10.1016/j.nimb.2011.03.027

Chabas A, Lombardo T, Cachier H (2007) Altération des verres à vitres en atmosphère urbaine. Pollut Atmos, numéro spécial:23–28

Chabas A, Fouqueau A, Attoui M, Alfaro SC, Petitmangin A, Bouilloux A, Saheb M, Coman A, Lombardo T, Grand N, Zapf P, Berardo R, Duranton M, Durand-Jolibois R, Jerome M, Pangui E, Correia JJ, Guillot I, Nowak S (2015) Characterisation of CIME, an experimental chamber for simulating interactions between materials of the cultural heritage and the environment. Environ Sci Pollut Res 22:19170–19183. https://doi.org/10.1007/s11356-015-5083-5

Collective (2011) Chapter 23: museums, galleries, archives and libraries. In: ASHRAE Handbook - HVAC Applications, SI edn. ASHRAE Research, pp 1–23. Available on https://www.academia.edu/22524538/2011_ASHRAE_HANDBOOK_HVAC_Applications_SI_Edition

Credou J, Berthelot T (2014) Cellulose : from biocompatible to bioactive material. J Mater Chem B 2:4767–4788. https://doi.org/10.1039/C4TB00431K

Davidson RS (1996) The photodegradation of some naturally occurring polymers. J Photochem Photobiol B 33:3–25. https://doi.org/10.1016/1011-1344(95)07262-4

Douthwaite FJ, Lewis DM, Schumacher-Hamedat U (1993) Reaction of cystine residues in wool with peroxy compounds. Text Res J 63:177–183. https://doi.org/10.1177/004051759306300308

Duffield PA, Lewis DM (1985) The yellowing and bleaching of wool. Rev Prog Color Relat Top 15:38–51. https://doi.org/10.1111/j.1478-4408.1985.tb03735.x

Dupont A-L (1996) Degradation of cellulose at the wet/dry interface. II. An Approach to the Identification of the Oxidation Compounds. Restaurator 17:145–164. https://doi.org/10.1515/rest.1996.17.3.145

Dupont A-L (2003) Cellulose in lithium chloride/N,N-dimethylacetamide, optimisation of a dissolution method using paper substrates and stability of the solutions. Polymer 44:4117–4126. https://doi.org/10.1016/S0032-3861(03)00398-7

Dupont A-L, Réau D, Bégin P, Paris-Lacombe S, Tétreault J, Mortha G (2018) Accurate molar masses of cellulose for the determination of degradation rates in complex paper samples. Carbohydr Polym 202:172–185. https://doi.org/10.1016/j.carbpol.2018.08.134

Dyer JM, Bringans SD, Bryson WG (2006) Characterisation of photo-oxidation products within photoyellowed wool proteins: tryptophan and tyrosine derived chromophores. Photochem Photobiol Sci 5: 698–706. https://doi.org/10.1039/B603030K

Edwards CJ, Hudson FL, Hockey JA (1968) Sorption of sulphur dioxide by paper. J Appl Chem 18:146–148. https://doi.org/10.1002/jctb.5010180506

Erra P, Gómez N, Dolcet LM, Juliá MR, Lewis DM, Willoughby JH (1997) FTIR analysis to study chemical changes in wool following a sulfitolysis treatment. Text Res J 67:397–401. https://doi.org/10.1177/004051759706700602

Evans R, Wallis A (1987) Comparison of cellulose molecular weights determined by high performance size exclusion chromatography and viscometry. In: Proceedings of the Fourth International Symposium on Wood and Pulping Chemistry, vol 1, Paris, pp 201–205

Florian MLE (1997) Heritage eaters: insects and fungi in heritage collections. James & James (Science Publishers) Ltd. https://doi.org/10.14288/1.0342857

Florian MLE, Kronkright DP, Norton RE (1991) The conservation of artifacts made from plant materials. Getty Publications. Available on https://www.getty.edu/conservation/publications_resources/pdf_publications/pdf/cons_artifacts.pdf

Fuzek JF (1985) Absorption and desorption of water by some common fibers. Ind Eng Chem Prod Res Dev 24:140–144. https://doi.org/10.1021/i300017a026

Gómez N, Juliá MR, Lewis DM, Erra P (1995) The use of FTIR to investigate modifications to wool treated with sodium sulphite and cationic protein hydrolysate. J Soc Dye Colour 111:281–284. https://doi.org/10.1111/j.1478-4408.1995.tb01742.x

Grau-Bové J, Strlič M (2013) Fine particulate matter in indoor cultural heritage: a literature review. Herit Sci 1:8. https://doi.org/10.1186/2050-7445-1-8

Grau-Bové J, Budič B, Cigić IK, Thickett D, Signorello S, Strlič M (2016) The effect of particulate matter on paper degradation. Herit Sci 4:2. https://doi.org/10.1186/s40494-016-0071-8

Grzywacz CM (2006) Monitoring for gaseous pollutants in museums. The Getty Conservation Institute. Available on http://www.getty.edu/conservation/publications_resources/pdf_publications/pdf/monitoring.pdf

Hajji L, Boukir A, Assouik J, Pessanha S, Figueirinhas JL, Carvalho ML (2016) Artificial aging paper to assess long-term effects of conservative treatment. Monitoring by infrared spectroscopy (ATR-FTIR), X-ray diffraction (XRD), and energy dispersive X-ray fluorescence (EDXRF). Microchem J 124:646–656. https://doi.org/10.1016/j.microc.2015.10.015

Havermans J, Dufour J (1997) Photo oxidation of paper documents A literature reviews. Restaurator 18:103–114. https://doi.org/10.1515/rest.1997.18.3.103

Hietala J, Vuori A, Johnsson P et al (2016) Formic acid. In: Ullmann's Encyclopedia of Industrial Chemistry. American Cancer Society, pp 1–22. https://doi.org/10.1002/14356007.a12_013.pub3

Hill CAS, Norton A, Newman G (2009) The water vapor sorption behavior of natural fibers. J Appl Polym Sci 112:1524–1537. https://doi.org/10.1002/app.29725

Hudson FL, Milner WD (1961) The permanence of paper. The use of radioactive sulphur to study the pick-up of sulphur dioxide by paper. Pap Technol 2:155–161

Inglis AS, Liu T-Y (1970) The stability of cysteine and cystine during acid hydrolysis of proteins and peptides. J Biol Chem 245:112–116

Iqbal M, Sohail M, Ahmed A et al (2012) Textile environmental conditioning: effect of relative humidity variation on the tensile properties of different fabrics. J Anal Sci Methods Instrum 2:92

Johansson A, Lennholm H (2000) Influences of SO2 and O3 on the ageing of paper investigated by in situ diffuse reflectance FTIR and time-resolved trace gas analysis. Appl Surf Sci 161:163–169. https://doi.org/10.1016/S0169-4332(00)00277-4

Johansson A, Kolseth P, Lindqvist O (2000) Uptake of air pollutants by paper. Restaurator 21:117–137. https://doi.org/10.1515/REST.2000.117

Kang GD, Lee KH, Ki CS, Park YH (2004) Crosslinking reaction of phenolic side chains in silk fibroin by tyrosinase. Fibers Polym 5: 234–238. https://doi.org/10.1007/BF02903006

Karpowicz A (1981) Ageing and deterioration of proteinaceous media. Stud Conserv 26:153–160. https://doi.org/10.1179/sic.1981.26.4.153

Kavkler K, Gunde-Cimerman N, Zalar P, Demšar A (2011) FTIR spectroscopy of biodegraded historical textiles. Polym Degrad Stab 96: 574–580. https://doi.org/10.1016/j.polymdegradstab.2010.12.016

Kissi N, Curran K, Vlachou-Mogire C, Fearn T, McCullough L (2017) Developing a non-invasive tool to assess the impact of oxidation on the structural integrity of historic wool in Tudor tapestries. Herit Sci 5:49. https://doi.org/10.1186/s40494-017-0162-1

Knill CJ, Kennedy JF (2003) Degradation of cellulose under alkaline conditions. Carbohydr Polym 51:281–300. https://doi.org/10.1016/S0144-8617(02)00183-2

Kobayashi Y, Yoshizumi K (1994) Soiling and deterioration of wool fiber due to exposure to atmospheric environment. Sen'i Gakkaishi 50:402–405

Koperska MA, Pawcenis D, Bagniuk J, Zaitz MM, Missori M, Łojewski T, Łojewska J (2014) Degradation markers of fibroin in silk through infrared spectroscopy. Polym Degrad Stab 105:185–196. https://doi.org/10.1016/j.polymdegradstab.2014.04.008

Koperska MA, Łojewski T, Łojewska J (2015) Evaluating degradation of silk's fibroin by attenuated total reflectance infrared spectroscopy: case study of ancient banners from Polish collections. Spectrochim Acta A Mol Biomol Spectrosc 135:576–582. https://doi.org/10.1016/j.saa.2014.05.030

Korenberg C (2007) The effect of ultraviolet-filtered light on the mechanical strength of fabrics. Tech Res Bull - Br Mus 1:23–27

Koura A, Krause T (2013) Increase of paper permanence by treatment with liquid ammonia or ammonia solutions: Part I, Fundamental basis and influence on fibre and paper structure and properties. In: Petherbridge G (ed) Conservation of library and archive materials and the graphic arts. Elsevier, pp 31–36. Available on https://sisis.rz.htw-berlin.de/inhalt/0122550.pdf

Koussoulou T (1999) Photodegradation and photostabilization of historic silks in the museum environment – evaluation of a new conservation treatment. Pap Inst Archaeol 10:75–88. https://doi.org/10.5334/pia.135

Launer HF (1971) Rapid Bleaching of Wool With Extremely Intense Visible Light. Text Res J 41:311–314. https://doi.org/10.1177/004051757104100404

Lennard F, Dulieu-Barton JM (2014) Quantifying and visualizing change: strain monitoring of tapestries with digital image correlation. Stud Conserv 59:241–255. https://doi.org/10.1179/2047058413Y.0000000097

Łojewska J, Miśkowiec P, Łojewski T, Proniewicz LM (2005) Cellulose oxidative and hydrolytic degradation: in situ FTIR approach. Polym Degrad Stab 88:512–520. https://doi.org/10.1016/j.polymdegradstab.2004.12.012

Łojewski T, Zięba K, Knapik A, Bagniuk J, Lubańska A, Łojewska J (2010) Evaluating paper degradation progress. Cross-linking between chromatographic, spectroscopic and chemical results. Appl Phys A Mater Sci Process 100:809–821. https://doi.org/10.1007/s00339-010-5657-5

Margutti S, Vicini S, Proietti N, Capitani D, Conio G, Pedemonte E, Segre AL (2002) Physical-chemical characterisation of acrylic polymers grafted on cellulose. Polymer 43:6183–6194

Margutti S, Conio G, Calvini P, Pedemonte E (2008) Hydrolytic and oxidative degradation of paper. Restaurator 22:67–83. https://doi.org/10.1515/REST.2001.67

Mellet P, Louw DF (1965) The modification of silk fibroin by alkali. Chem Commun Lond:396b–3397b. https://doi.org/10.1039/C1965000396B

Menart E, De Bruin G, Strlič M (2011) Dose–response functions for historic paper. Polym Degrad Stab 96:2029–2039. https://doi.org/10.1016/j.polymdegradstab.2011.09.002

Menart E, de Bruin G, Strlič M (2014) Effects of NO2 and acetic acid on the stability of historic paper. Cellulose 21:3701–3713. https://doi.org/10.1007/s10570-014-0374-4

Michalski S (1993) Relative humidity: a discussion of correct/incorrect values. In: Preprints. International Council of Museums Committee for Conservation, Washinghton DC, 22-27 August 1993, pp 624–629. Available on https://www.icom-cc-publications-online.org/2820/Relative-Humidity%2D%2DA-Discussion-of-CorrectIncorrect-Values

Millington KR, Church JS (1997) The photodegradation of wool keratin II. Proposed mechanisms involving cystine. J Photochem Photobiol B 39:204–212. https://doi.org/10.1016/S1011-1344(96)00020-6

Miyazaki T (1984) Adsorption characteristics of NOx by several kinds of interior materials. Indoor Air Chem Charact Pers Expo 4:103–110

Norton GP, Nicholls CH (1967) Some chemical reactions involved in the alkaline yellowing of wool. Text Res J 37:1031–1037. https://doi.org/10.1177/004051756703701205

Odlyha M, Theodorakopoulos C, Campana R (2007) Studies on woolen threads from historical tapestries. AUTEX Res J 7:9–18

Otterburn MS (1977) The chemistry and reactivity of silk. In: Asquith RS (ed) Chemistry of Natural Protein Fibers. Springer US, Boston, MA, pp 53–80

Paquin R, Colomban P (2007) Nanomechanics of single keratin fibres: a Raman study of the a-helix →b-sheet transition and the effect of water. J Raman Spectrosc 38:504–514. https://doi.org/10.1002/jrs.1672

Pavasars I, Hagberg J, Borén H, Allard B (2003) Alkaline degradation of cellulose: mechanisms and kinetics. J Polym Environ 11:39–47. https://doi.org/10.1023/A:1024267704794

Pawcenis D, Smoleń M, Aksamit-Koperska MA, Łojewski T, Łojewska J (2016) Evaluating the impact of different exogenous factors on silk textiles deterioration with use of size exclusion chromatography. Appl Phys A Mater Sci Process 122:576. https://doi.org/10.1007/s00339-016-0052-5

Phillips GO, Arthur JC (1964) Chemical effects of light on cotton cellulose and related compounds: part ii: photodegradation of cotton cellulose. Text Res J 34:572–580. https://doi.org/10.1177/004051756403400702

Posati T, Sotgiu G, Varchi G et al (2016) Developing keratin sponges with tunable morphologies and controlled antioxidant properties induced by doping with polydopamine (PDA) nanoparticles. Mater Des 110:475–484. https://doi.org/10.1016/j.matdes.2016.08.017

Ramsay GC (1970) Yellowing of wool. Wool Sci Rev 39:27–39

Rousseau M-E, Lefèvre T, Beaulieu L, Asakura T, Pézolet M (2004) Study of protein conformation and orientation in silkworm and spider silk fibers using Raman microspectroscopy. Biomacromolecules 5:2247–2257. https://doi.org/10.1021/bm049717v

Schieweck A, Salthammer T (2009) Emissions from construction and decoration materials for museum showcases. Stud Conserv 54:218–235. https://doi.org/10.1179/sic.2009.54.4.218

Seves A, Romanò M, Maifreni T, Sora S, Ciferri O (1998) The microbial degradation of silk: a laboratory investigation. Int Biodeterior Biodegrad 42:203–211. https://doi.org/10.1016/S0964-8305(98)00050-X

Shao JZ, Zheng JH, Liu JQ, Carr CM (2005) Fourier transform Raman and Fourier transform infrared spectroscopy studies of silk fibroin. J Appl Polym Sci 96:1999–2004. https://doi.org/10.1002/app.21346

Shaw JTB (1964) Fractionation of the fibroin of Bombyx mori with alkali. Biochem J 93:54–61

Sistach MC, Ferrer N, Romero MT (1998) Fourier transform infrared spectroscopy applied to the analysis of ancient manuscripts. Restaurator 19:173–186. https://doi.org/10.1515/rest.1998.19.4.173

Socrates G (2004) Infrared and Raman characteristic group frequencies: tables and charts. John Wiley & Sons. 3rd edition. 366 pp

Spicer CW, Kenny DV, Ward GF, Billick IH (1993) Transformations, lifetimes, and sources of NO2, HONO, and HNO3 in indoor environments. Air Waste 43:1479–1485. https://doi.org/10.1080/1073161X.1993.10467221

Strlič M, Kralj Cigić I, Možir A, de Bruin G, Kolar J, Cassar M (2011) The effect of volatile organic compounds and hypoxia on paper degradation. Polym Degrad Stab 96:608–615. https://doi.org/10.1016/j.polymdegradstab.2010.12.017

Sugihara JM (1953) Relative reactivities of hydroxyl groups of carbohydrates. Adv Carbohydr Chem 8:1–44. https://doi.org/10.1016/S0096-5332(08)60097-1

Sun Y, Lin L, Pang C, Deng H, Peng H, Li J, He B, Liu S (2007) Hydrolysis of cotton fiber cellulose in formic acid. Energy Fuel 21:2386–2389. https://doi.org/10.1021/ef070134z

Szostak-Kotowa J (2004) Biodeterioration of textiles. Int Biodeterior Biodegrad 53:165–170. https://doi.org/10.1016/S0964-8305(03)00090-8

Taddei P, Arosio C, Monti P, Tsukada M, Arai T, Freddi G (2007) Chemical and physical properties of sulfated silk fabrics. Biomacromolecules 8:1200–1208. https://doi.org/10.1021/bm061017y

Tétreault J (2003) Polluants dans les musées et les archives - évaluation des risques, stratégies de contrôle et gestion de la préservation. Canadian Conservation Institute, 174 pp

Tétreault J, Dupont A-L, Bégin P, Paris S (2013) The impact of volatile compounds released by paper on cellulose degradation in ambient hygrothermal conditions. Polym Degrad Stab 98:1827–1837. https://doi.org/10.1016/j.polymdegradstab.2013.05.017

Timar-Balazsy A, Eastop D (2012) Chemical principles of textile conservation, Hoboken:Taylor and Francis. Numerical version. First edition in 1998. Routledge

Tsuge S, Yokoi H, Ishida Y, Ohtani H, Becker MA (2000) Photodegradative changes in chemical structures of silk studied by pyrolysis–gas chromatography with sulfur chemiluminescence detection. Polym Degrad Stab 69:223–227. https://doi.org/10.1016/S0141-3910(00)00067-7

Upham JB, Salvin VS (1975) Effects of air pollutants on textile fibers and dyes. Environmental Protection Agency, USA

Uring P, Chabas A, De Reyer D et al (2018) The Bayeux embroidery: a dust deposition assessment. Herit Sci 6:23. https://doi.org/10.1186/s40494-018-0190-5

Uring P, Chabas A, Alfaro S (2019) Dust deposition on textile and its evolution in indoor cultural heritage. Eur Phys J Plus 134:255. https://doi.org/10.1140/epjp/i2019-12671-5

Uring P, Chabas A, Alfaro S, Derbez M (2020) Assessment of indoor air quality for a better preventive conservation of some French museums and monuments. Environ Sci Pollut Res Int 27:42850–42867. https://doi.org/10.1007/s11356-020-10257-6

Vichi F, Mašková L, Frattoni M, Imperiali A, Smolík J (2016) Simultaneous measurement of nitrous acid, nitric acid, and nitrogen dioxide by means of a novel multipollutant diffusive sampler in libraries and archives. Herit Sci 4:4. https://doi.org/10.1186/s40494-016-0074-5

Vilaplana F, Nilsson J, Sommer D, Karlsson S (2015) Analytical markers for silk degradation: comparing historic silk and silk artificially aged in different environments. Anal Bioanal Chem 407:1433–1449. https://doi.org/10.1007/s00216-014-8361-z

Walsh M, Black A, Morgan A, Crawshaw GH (1977) Sorption of SO2 by typical indoor surfaces including wool carpets, wallpaper and paint.

Atmos Environ 1967(11):1107–1111. https://doi.org/10.1016/0004-6981(77)90242-6

Watt J, Hamilton R (2003) The soiling of buildings by air pollution. In: Brimblecombe P (ed) The Effects of Air Pollution on the Built Environment. Imperial College Press, London, pp 289–334

Whitmore PM, Bogaard J (1994) Determination of the cellulose scission route in the hydrolytic and oxidative degradation of paper. Restaurator 15:26–45. https://doi.org/10.1515/rest.1994.15.1.26

Williams EL, Grosjean D (1992) Exposure of deacidified and untreated paper to ambient levels of sulfur dioxide and nitrogen dioxide: nature and yields of reaction products. J Am Inst Conserv 31:199–212. https://doi.org/10.1179/019713692806066655

Wojciechowska E, Włochowicz A, Wesełucha-Birczyńska A (1999) Application of Fourier-transform infrared and Raman spectroscopy to study degradation of the wool fiber keratin. J Mol Struct 511–512: 307–318. https://doi.org/10.1016/S0022-2860(99)00173-8

Wojciechowska E, Włochowicz A, Wesełucha-Birczyńska A (2000) Application of Fourier-transform infrared and Raman spectroscopy to the study of the influence of orthosilicic acid on the structure of wool fibre. J Mol Struct 555:397–406. https://doi.org/10.1016/S0022-2860(00)00626-8

Zhao H, Kwak JH, Conrad Zhang Z et al (2007) Studying cellulose fiber structure by SEM, XRD, NMR and acid hydrolysis. Carbohydr Polym 68:235–241. https://doi.org/10.1016/j.carbpol.2006.12.013